Available online at www.sciencedirect.com

SciVerse ScienceDirect

Ceramics International 38 (2012) 4991–4995

CERAMICS INTERNATIONAL

www.elsevier.com/locate/ceramint

The influence of Mo^{6+} doping on the luminescence properties of red-emitting phosphor $Sr_9Eu_2W_{4-x}Mo_xO_{24}$ ($x = 0$–4)

Xigang Wang [a], Yanlin Huang [a,*], Young Moon Yu [b], Sun Il Kim [c], Hyo Jin Seo [c,*]

[a] College of Chemistry, Chemical Engineering and Materials Science, Soochow University, Suzhou 215123, China
[b] LED-Marin Convergence Technology R&BD Center, Pukyong National University, Busan 608-739, Republic of Korea
[c] Department of Physics, Pukyong National University, Busan 608-737, Republic of Korea

Received 28 January 2012; received in revised form 28 February 2012; accepted 28 February 2012
Available online 10 March 2012

Abstract

A series of red emitting phosphors $Sr_9Eu_2W_{4-x}Mo_xO_{24}$ ($x = 0$–4) have been synthesized by solid-state reactions and their crystal structures, photoluminescence properties were studied. The excitation and emission spectra of $Sr_9Eu_2W_{4-x}Mo_xO_{24}$ phosphors can be modified by Mo^{6+} doping. As the molybdate content increased, the Eu^{3+} emission intensity of $Sr_9Eu_2W_{4-x}Mo_xO_{24}$ ($x = 0$–4) under 395 nm excitation was found to increase and reached a maximum at $x = 2$. The excitation spectra, the emission intensities and the chromaticity coordinates of $Sr_9Eu_2W_{4-x}Mo_xO_{24}$ ($x = 2$) were compared to those of the conventional red phosphor Y_2O_2S: Eu^{3+}. The intense red-emission under near-UV excitation suggests that $Sr_9Eu_2W_{4-x}Mo_xO_{24}$ ($x = 2$) could be a potential candidate for white light generation by using near-UV LEDs. In this study, the effects of Mo^{6+} doping on the crystal structure and photoluminescence properties of $Sr_9Eu_2W_{4-x}Mo_xO_{24}$ were discussed.
© 2012 Elsevier Ltd and Techna Group S.r.l. All rights reserved.

Keywords: Optical materials and properties; White LEDs; Rare-earth compounds; Europium

1. Introduction

Solid state lighting based on inorganic white light-emitting diodes (W-LEDs) has been intensively investigated for replacing the conventional incandescent and fluorescent lamps due to their excellent properties, for example, high luminous efficiency, low power consumption, environmentally friendly features, reliability, and long life time (100,000 h) [1,2]. The performance of W-LEDs depends on the luminescence properties of the phosphors. Accordingly, the investigations of new efficient phosphors for W-LEDs have gained much attention [3–6]. In particular, Eu^{3+}-doped compounds are of strong interests for the application in W-LEDs with near UV and blue LEDs chips [7].

One of the commonly used red-emitting phosphors is Eu^{3+}-doped Y_2O_2S, which is chemically unstable (releasing of hydrogen sulfide gas) and its fluorescent efficiency is lower than that of the blue ($BaMgAl_{10}O_{17}$:Eu^{2+}) and green-emitting (ZnS:Cu^{+}, Al^{3+}) phosphors [8]. The other red-emitting phosphors also have some disadvantages, e.g., sulfide-based phosphor CaS:Eu^{2+} shows luminescence saturation with an increasing applied current when it is incorporated into phosphor-converted W-LEDs' devices [9]. Although Eu^{2+}- or Ce^{3+}-doped nitrides are efficient red-emitting phosphors, the very high firing temperature and high nitrogen pressure in the synthesis lead to higher production cost [10]. The investigations of new efficient red-emitting phosphors for W-LEDs have received more attention. The red emitting at 610–615 nm is the best choice for a fluorescent light source with respect to luminous efficiency and color rendering [11].

As important optical materials, Eu^{3+} ions doped tungstates have been widely investigated due to its wonderful red-emitting characteristics. Recently, Zeng et al. have reported the luminescence properties of Eu^{3+}-fully concentrated $Sr_9Eu_2W_4O_{24}$ [12,13]. This phosphor shows the excellent luminescent properties on excitation at 395 and 465 nm. The bright red-LEDs and white-LEDs are fabricated by combining the phosphor with 395 nm-emitting InGaN and 460 nm-emitting InGaN chips. What makes $Sr_9Eu_2W_4O_{24}$ special is

* Corresponding authors.
E-mail addresses: huang@suda.edu.cn (Y. Huang), hjseo@pknu.ac.kr (H.J. Seo).

0272-8842/$36.00 © 2012 Elsevier Ltd and Techna Group S.r.l. All rights reserved.
doi:10.1016/j.ceramint.2012.02.094

that the luminescence of Eu^{3+} has no concentration quenching even though the host is fully Eu-concentrated. This is very favorable for the applications in W-LEDs because it can suffer from high photon flux during its application without luminescence quenching. $Sr_9Eu_2W_4O_{24}$ could be potential red component for near-UV based three-band WLEDs and commercial blue-emitting InGaN-based YAG:Ce^{3+} WLEDs [12,13].

This work gives insight into the luminescence properties of the red emitting phosphor $Sr_9Eu_2W_4O_{24}$ by Mo^{6+} doping. The phosphors of $Sr_9Eu_2W_{4-x}Mo_xO_{24}$ ($x = 0$–4) were synthesized by solid-state reaction. The photoluminescence excitation and emission spectra together with the luminescence decay curves were investigated. The luminescence properties were evaluated to investigate the possible application in W-LEDs phosphors.

2. Experimental

$Sr_9Eu_2W_{4-x}Mo_xO_{24}$ ($x = 0$–4) were prepared by solid state reaction at high temperature. The starting materials were Eu_2O_3 (99.99%), $SrCO_3$ (99.9%), WO_3 (99.9%)and MoO_3 (99.9%). The stoichiometric raw materials were weighed and thoroughly mixed in an agate mortar, then transferred to a corundum crucible and heated at 850, 1100 and 1350 °C for 10 h in air, respectively.

The XRD were collected on a Rigaku D/Max diffractometer operating at 40 kV, 30 mA with Bragg–Brentano geometry using Cu Ka radiation (λ = 1.54056 Å). The excitation and luminescence spectra were recorded on a Perkin-Elmer LS-50B luminescence spectrometer with Monk–Gillieson type monochromators and a xenon discharge lamp used as the excitation source. The luminescence decay curves were measured by the excitation of 355 nm pulsed Nd:YAG laser (Spectron Laser Sys. SL802G). The signals were recorded by the 500 MHz digital oscilloscope (Tektronix DPO 3054).

3. Results and discussion

Fig. 1 shows the XRD patterns of $Sr_9Eu_2W_{4-x}Mo_xO_{24}$ ($x = 0$–4) phosphors. The peak positions and the relative intensities of the XRD patterns are the same as the PDF2 standard cards selected in the International Centre for Diffraction Data (ICDD) database: No. 50-0375 for $Sr_9Gd_2W_4O_{24}$. No impurity line was observed. The sharp peaks in each XRD pattern indicate good crystallizability of the samples.

To the best of our knowledge, there is no structural data reported for $Sr_9Eu_2Mo_4O_{24}$ up to now. So the XRD pattern of $Sr_9Eu_2Mo_4O_{24}$ was fitted by Jade. 5.0 program by taking $Sr_9Gd_2W_4O_{24}$ (PDF2 Card No. 50-0375) in Fig. 1 as the reference. The similarity of the diffraction patterns clearly shows that two samples are isostructural. All the peaks in the XRD patterns were well indexed with the $Sr_9Gd_2W_4O_{24}$ perovskite structure. In the series of $Sr_9Eu_2W_{4-x}Mo_xO_{24}$ ($x = 0$–4), the cell parameter a decreases continuously with increasing Mo^{6+} concentration x, which reveals that the series form whole range solid solutions.

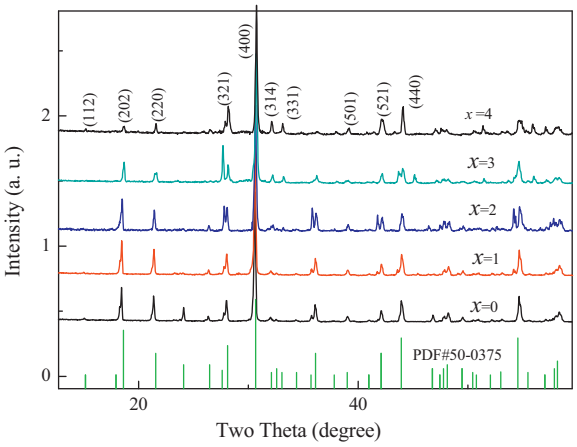

Fig. 1. XRD patterns of $Sr_9Eu_2W_{4-x}Mo_xO_{24}$ ($x = 0$–4) of this work and PDF2 Card No. 350-0375.

Fig. 2 is the corresponding schematic views of $Sr_9Eu_2W_4O_{24}$ structure. $Sr_9Eu_2W_4O_{24}$ shows polymorphic phase transformation of perovskite-type structure [14–16]. Sr^{2+} (called A-site) ions are coordinated to 12 oxygen atoms and M/W^{6+} ($M = Eu^{3+} + Sr^{2+}$) ions (coordinated to 6 oxygen atoms) are ordered in the B-site. M sites are randomly occupied by $0.5Sr^{2+} + 0.5Eu^{3+}$. The crystal structure consists of a cubic closely packed array of Sr–O layers wherein W and M atoms are ordered and face centered, which has its origin in an ordering of cationic vacancies. A large size difference between W and M atoms ($Eu^{3+} + Sr^{2+}$) favors the long range of crystalline structure in the B site ordering.

As shown in Fig. 2, the shortest distances between the two adjacent Eu^{3+} ions in $Sr_9Eu_2W_4O_{24}$ is 5.826 Å. The distance is much longer than the reported values in some fully Eu-concentrated phosphors without any concentration quenching, for example, the shortest Eu^{3+}–Eu^{3+} distance is 3.8801 Å in Eu_3BWO_9 [17], and 4.9 Å in $EuBaB_9O_{16}$ [18]. The long Eu^{3+}–Eu^{3+} distances in $Sr_9Eu_2W_4O_{24}$ can hamper the energy migration among Eu^{3+} ions. Eu^{3+} ions in $Sr_9Eu_2W_4O_{24}$ are all surrounded by the big WO_6 octahedra and located in an isolated site with a long distance. Consequently, there is no

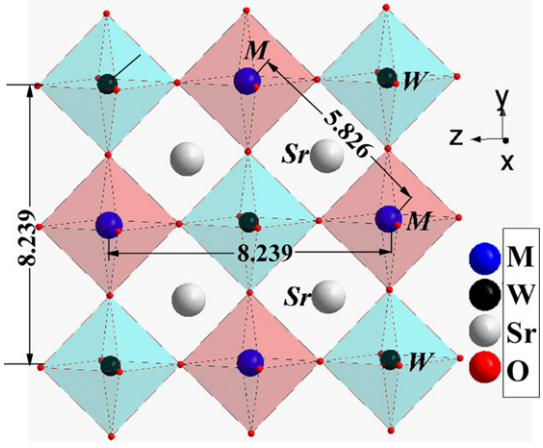

Fig. 2. the schematic structure views of the $Sr_9Eu_2W_4O_{24}$ along the [0 0 1] direction. $M = 0.5Eu^{3+} + 0.5Sr^{2+}$. The numbers in the figure show the distances (unit in Å) between the adjacent M and W(Mo) ions in the lattices.

concentration quenching in Eu^{3+}-doped $Sr_9Gd_{2-x}Eu_xW_4O_{24}$ as reported by Zeng et al. [12,13], and the strongest luminescence is found in the Eu^{3+}-fully concentrated $Sr_9Eu_2W_4O_{24}$.

Fig. 3(a) shows the photoluminescence excitation spectra of $Sr_9Eu_2W_{4-x}Mo_xO_{24}$ ($x = 0$–4). The excitation spectra of $Sr_9Eu_2W_4O_{24}$ ($x = 0$) by monitoring the $^5D_0 \rightarrow {}^7F_2$ emission (618 nm) of Eu^{3+} consist of a broad band and some sharp lines. The broad excitation band can be attributed to the O→W ligand-to-metal charge-transfer (CT) transition [19]. The CT band of Eu^{3+}–O^{2-} was not clearly observed, which could be due to an overlap with that of tungstate group. In the range from 350 to 460 nm, $Sr_9Eu_2W_4O_{24}$ presents the characteristic intra-configurational 4f–4f transitions of Eu^{3+}: 395 nm ($^7F_0 \rightarrow {}^5L_6$) and 464 nm ($^7F_0 \rightarrow {}^5D_2$).

With increasing Mo^{6+} doping in $Sr_9Eu_2W_{4-x}Mo_xO_{24}$ ($x = 0$–4) (Fig. 3a), the excitation spectra of the broad bands around 400 nm, move to long wavelength and overlap with some f–f transitions of Eu^{3+}. In Mo-rich phases ($x = 2$–4) the f–f-transitions of Eu^{3+} cannot be clearly determined. The broad bands should originate from the CTs of MoO_6, WO_6 and Eu^{3+}–O^{2-}. Usually, the CT band of the MoO_6 group covers the range 350–450 nm and that of the WO_6 group locates around 250–350 nm in tungstates and molydates with peverskite-type structure [20]. So this red-shift of CT band is attributed to the absorption of Mo^{6+} ions. This is beneficial to white-LEDs because it well matches with the output wavelength of near-UV or blue LED chips in phosphor-converted W-LEDs.

Fig. 3(b) is the comparison of excitation spectra between $Sr_9Eu_2W_{4-x}Mo_xO_{24}$ ($x = 2$) ($\lambda_{em} = 618$ nm) and the red-emitting phosphor $Y_2O_2S{:}Eu^{3+}$ ($\lambda_{em} = 627$ nm). On the excitation spectrum of $Y_2O_2S{:}Eu^{3+}$, the strong broad band before 350 nm corresponds to CT transition of the Eu–O and Eu^{3+}–S^{2-} [21]. However, the absorption in the near-ultraviolet or blue region is very weak.

Fig. 4(a) presents the luminescence spectra of $Sr_9Eu_2W_{4-x}Mo_xO_{24}$ ($x = 0$–4) under 395 nm excitation at 300 K. These phosphors have similar PL emission spectra. Upon the excitation with 395 nm, the emission spectra of $Sr_9Eu_2W_{4-x}Mo_xO_{24}$ ($x = 0$–4) display $^5D_0 \rightarrow {}^7F_J$ ($J = 0$–4) emission lines of the Eu^{3+} ions. The dominant red emission of 618 nm in Fig. 4(a) is attributed to the electric dipole transition $^5D_0 \rightarrow {}^7F_2$, indicating that Eu^{3+} ions are located at the site of non-inversion symmetry. This is in agreement with the crystal structure, i.e., Eu^{3+} ions in $Sr_9Eu_2W_{4-x}Mo_xO_{24}$ lattices are located on the *M* sites which are randomly occupied by 0.5 Sr^{2+} and 0.5Eu^{3+} ions.

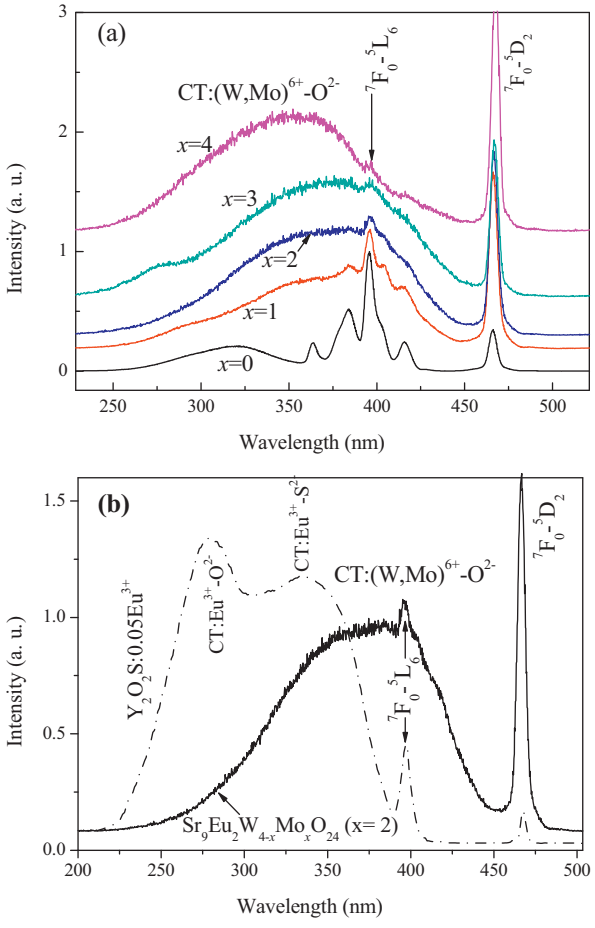

Fig. 3. The excitation spectra of $Sr_9Eu_2W_{4-x}Mo_xO_{24}$ ($x = 0$–4) (a) and the comparison of excitation spectra between $Sr_9Eu_2W_{4-x}Mo_xO_{24}$ ($x = 2$) ($\lambda_{em} = 618$ nm) and the red-emitting phosphor $Y_2O_2S{:}Eu^{3+}$ ($\lambda_{em} = 627$ nm) (b).

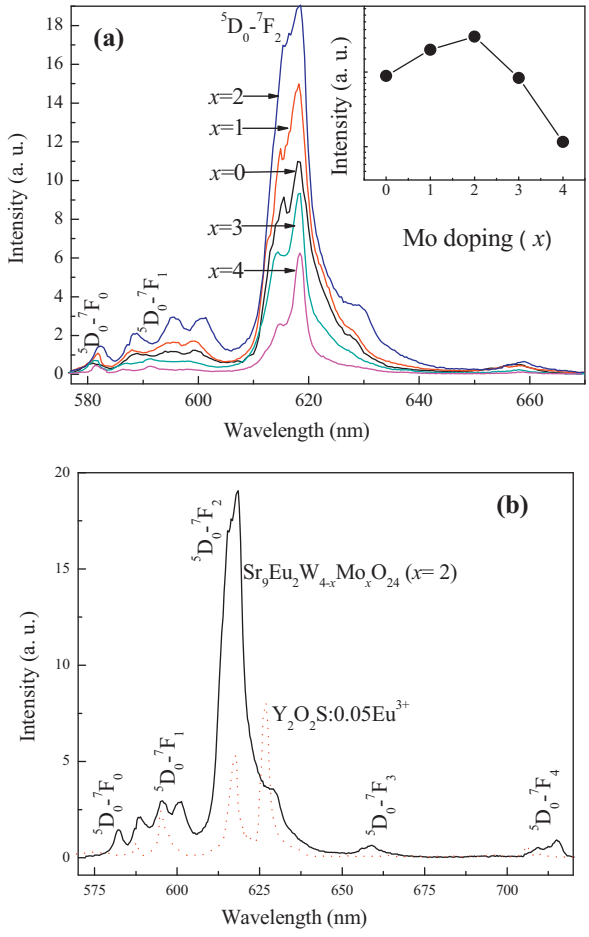

Fig. 4. (a) The luminescence spectra of $Sr_9Eu_2W_{4-x}Mo_xO_{24}$ ($x = 0$–4) under 395 nm excitation at 300 K. Inset is a plot of integrated intensity as a function of doping concentration of Mo^{6+} ions and (b) the luminescence spectra of $Sr_9Eu_2W_{4-x}Mo_xO_{24}$ ($x = 2$) $Y_2O_2S{:}0.05Eu^{3+}$ ($\lambda_{ex} = 395$ nm).

Inset in Fig. 4(a) is a plot of integrated intensity as a function of doping concentration of Mo^{6+} ions. Under 395 nm excitation, the luminescence intensity increases with increasing the Mo^{6+}-doping until a maximum intensity at $x = 2$, and then the luminescence intensity decreases. $Sr_9Eu_2W_{4-x}Mo_xO_{24}$ ($x = 2$) presents the strongest luminescence intensity among this series of phosphors.

Upon the excitation with 395 nm, the main emission lines of $Y_2O_2S:Eu^{3+}$ in Fig. 4(b) are 594 and 627 nm corresponding to the $^5D_0 \rightarrow {}^7F_1$ and $^5D_0 \rightarrow {}^7F_2$, respectively. And the integral emission intensity of $Sr_9Eu_2W_{4-x}Mo_xO_{24}$ ($x = 2$), which is proportional to the quantum efficiency, is 3.41 times higher than that of $Y_2O_2S:Eu^{3+}$ under the same measurement conditions (excitation 395 nm). The CIE color values of $Sr_9Eu_2W_{4-x}Mo_xO_{24}$ ($x = 2$) are ($x = 0.66$, $y = 0.35$), which are closer to the standard of National Television Standards Committee ($x = 0.67$, $y = 0.33$) than that of a commercial red phosphor of $Y_2O_2S:Eu^{3+}$ ($x = 0.622$, $y = 0.351$) [22]. Recently, Eu^{3+}-doped perovskites, for example, Eu^{3+}-doped $CaTiO_3$ [23] and A_2CaMO_6 (A = Sr, Ba; M = Mo, W) [24–27], have been widely investigated as potential phosphors for W-LEDs. The emission intensity of Eu^{3+}-doped Sr_2CaMoO_6 is reported to be 1.5 times higher than that of commercial $Y_2O_2S:Eu^{3+}$ [24]; $Sr_{1.5}Eu_{0.05}Li_{0.05}Ba_{0.4}CaWO_6$ has 4.5 times stronger luminescence intensity than that of commercial red phosphor (Nichia) under 465 nm excitation [25]. This suggests that Eu^{3+}-doped perovskites have potential application as phosphors for white light generation using blue/near-UV GaN-based W-LEDs [20,24].

The differences of $Sr_9Eu_2W_{4-x}Mo_xO_{24}$ luminescence from the reported Eu^{3+}-doped perovskites are of two aspects: firstly, the concentration of Eu^{3+} for the maximum intensity of $Sr_9Eu_2W_{4-x}Mo_xO_{24}$ (100%) is much higher than reported Eu^{3+}-doped perovskite phosphors; for example, the luminescence quenching concentration of the Eu^{3+} doping is only 3.0 mol% in $CaTiO_3:Eu^{3+}$ [23]; 5.0 mol% in $Sr_2ZnWO_6:Eu^{3+}$ [28] and 10 mol% in $Sr_2Ca_{1-2x}Eu_xNa_xMoO_6$ [25]. The high doping of Eu^{3+} ions in a phosphor can suffer high power excitation in the applications in W-LEDs. Secondly, the luminescence of $Sr_9Eu_2W_{4-x}Mo_xO_{24}$ is pure red-color due to strong $^5D_0 \rightarrow {}^7F_2$ transitions; it has been reported that Eu^{3+}-doped perovskites $Sr_2Ca_{0.8}Eu_{0.1}Na_{0.1}MoO_6$ [26,27] and $Ba_2Ca_{0.08}Eu_{0.02}MoO_6$ [20] give a sharp peak at 595 nm ascribed to the $^5D_0 \rightarrow {}^7F_1$ transition, which present origin-red color.

Usually in Eu^{3+}-doped tungastates, the band edge of absorption for WO_4 group locates at about 250–340 nm, and the excitation peaks at around 395 nm are owed to the f–f transitions of Eu^{3+}. The f–f transitions of Eu^{3+} are intrinsically spin- and parity-forbidden and their excitations could not be very efficient; with increasing the substitution of W^{6+} by Mo^{6+}, the average distance between MoO_6 decreases and the electron-delocalization among MoO_6 groups increases, thus the red-shift of the CT band of MoO_6 can be observed. With the replacement of W^{6+} by Mo^{6+} below $x < 2$, upon the excitation of near UV light the efficient energy transfer can take place from MoO_6 to Eu^{3+}. Thus under the excitation of 395 nm, the luminescence intensity of $Sr_9Eu_2W_{4-x}Mo_xO_{24}$ ($x = 1, 2$) was enhanced due to energy transfer from MoO_6 to Eu^{3+} ions. At the same time the energy transfer among MoO_6 is blocked because MoO_6 groups are separated by WO_6 and SrO_6 in $Sr_9Eu_2W_{4-x}Mo_xO_{24}$ lattices.

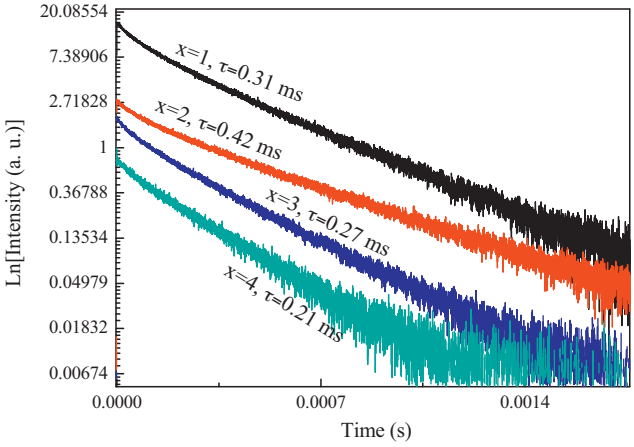

Fig. 5. The luminescence decay curves by monitoring 618 nm ($^5D_0 \rightarrow {}^7F_2$) in $Sr_9Eu_2W_{4-x}Mo_xO_{24}$ ($x = 1$–4) under 355 nm excitation at 300 K.

Generally, the luminescent emission of MoO_6 is very poor [29], e.g., Ba_2CaMoO_6 only presents very weak red luminescence even at low temperature 77 K [20]. This is due to the characteristics of MoO_6 groups: in Mo-rich hosts, the energy absorbed by the MoO_6 groups are strongly quenched by the energy transfer along MoO_6 framework by the exchange-mechanism [30]. In this mechanism, the critical distance of the related metal ions for the transfer should be short. In the perovskite compound Ba_2CaMoO_6, the critical distance of 8 Å is estimated for the transfer between MoO_6 and MoO_6 [20,31]. As shown in Fig. 2, the MoO_6–MoO_6 distances are calculated about 5.826 Å and 8.236 Å, the energy transfers related to the MoO_6 groups are reasonable. With increasing Mo^{6+} doping in $Sr_9Eu_2W_{4-x}Mo_xO_{24}$ ($x = 3$, 4), the absorbed energy of MoO_6 transfers along MoO_6 framework, it is greatly quenched. This results in little energy transference to the luminescent centre Eu^{3+}. This is the reason that the PL intensity decrease when more Mo^{6+} is doped in the lattices as shown in Fig. 4(a).

Fig. 5 presents the luminescence decay curves by monitoring 618 nm ($^5D_0 \rightarrow {}^7F_2$) in $Sr_9Eu_2W_{4-x}Mo_xO_{24}$ ($x = 0$–4) under 355 nm excitation at 300 K. The phosphor of $Sr_9Eu_2W_4O_{24}$ presents nearly exponential decay with lifetime of 0.29 ms (figure omitted). With increasing Mo^{6+} doping the luminescence lifetimes increase and present the maximum value of 0.42 ms in $Sr_9Eu_2W_{4-x}Mo_xO_{24}$ ($x = 2$). The luminescence lifetimes decrease with increasing Mo^{6+} doping above $x > 2$ as shown in Fig. 5. This is in consistence with the changes of luminescence intensity shown in inset in Fig. 4(a).

4. Conclusions

$Sr_9Eu_2W_{4-x}Mo_xO_{24}$ ($x = 0$–4) were prepared by solid state reaction at high temperature. The samples form a complete solid solution for the Mo^{6+} doping ($x = 0$–4) and crystal in a perovskite-type structure. With increasing Mo^{6+} doping the CT excitation bands in $Sr_9Eu_2W_{4-x}Mo_xO_{24}$ greatly move to long

wavelength and present a broad absorption around 400 nm. $Sr_9Eu_2W_{4-x}Mo_xO_{24}$ ($x = 0$–4) present more efficient excitation in the near UV region than that of the commercial red-emitting phosphor $Y_2O_2S:Eu^{3+}$. The CIE color values of $Sr_9Eu_2W_{4-x}Mo_xO_{24}$ ($x = 2$) are ($x = 0.66$, $y = 0.35$). With the doping of Mo^{6+} below $x \leq 2$, the luminescence intensity of $Sr_9Eu_2W_{4-x}Mo_xO_{24}$ increases because of the efficient energy transfer from MoO_6 to Eu^{3+}. With increasing Mo^{6+} doping $x > 2$, the luminescence intensity of $Sr_9Eu_2W_{4-x}Mo_xO_{24}$ decreases due to the strong quenching of the energy transfer along MoO_6 framework, which results in little energy transference to the luminescent centre Eu^{3+} ions. The strongest luminescence is observed in Eu^{3+}-fully concentrated $Sr_9Eu_2W_{4-x}Mo_xO_{24}$ ($x = 2$), which is 3.41 times higher than that of $Y_2O_2S:Eu^{3+}$ under the excitation of 395 nm. $Sr_9Eu_2W_2Mo_2O_{24}$ can be a promising red component for WLEDs.

Acknowledgements

This work was supported by Mid-career Researcher Program through National Research Foundation of Korea (NRF) grant funded by the Ministry of Education, Science and Technology (MEST) (Project No. 2009-0078682), and the Industrial Strategic technology development program (Project No: 10037416, Establishment of infrastructure for LED-marine convergence technology support and technology development for commercialization) funded by the Ministry of Knowledge Economy (MKE, Korea), and by a project funded by the Priority Academic Program Development of Jiangsu Higher Education Institutions (PAPD).

References

[1] E.F. Schubert, J.K. Kim, Solid-state light sources getting smart, Sci. 308 (2005) 1274–1278.
[2] C.C. Lin, R.-S. Liu, Advances in phosphors for light-emitting diodes, J. Phys. Chem. Lett. 2 (2011) 1268–1277.
[3] F.W. Liu, C.H. Hsu, F.S. Chen, C.H. Lu, Microwave-assisted solvothermal preparation and photoluminescence properties of $Y_2O_3:Eu^{3+}$ phosphors, Ceram. Int. 38 (2012) 1577–1584.
[4] P. Rai, M.K. Song, H.M. Song, J.H. Kim, Y.S. Kim, I.H. Lee, Y.T. Yu, Synthesis, growth mechanism and photoluminescence of monodispersed cubic shape Ce doped YAG nanophosphor, Ceram. Int. 38 (2012) 235–242.
[5] H.Y. Chen, M.H. Weng, S.J. Chang, R.Y. Yang, Preparation of $Sr_2SiO_4:Eu^{3+}$ phosphors by microwave-assisted sintering and their luminescent properties, Ceram. Int. 38 (2012) 125–130.
[6] N.A. Dulina, T.G. Deineka, R.P. Yavetskiy, Z.P. Sergienko, A.G. Doroshenko, P.V. Mateychenko, O.M. Vovk, N.A. Matveevskaya, Comparison of dispersants performance on the suspension $Lu_2O_3:Eu^{3+}$ stability and high-density compacts on their basis, Ceram. Int. 37 (2011) 1645–1651.
[7] Y.C. Fang, S.Y. Chu, P.C. Kao, Y.M. Chuang, Z.L. Zeng, Energy transfer and thermal quenching behaviors of $CaLa_2(MoO_4)4:Sm^{3+}$, Eu^{3+} red phosphors, J. Electrochem. Soc. 158 (2011) J1–J5.
[8] S. Neeraj, N. Kijima, A.K. Cheetham, Novel red phosphors for solid-state lighting: the system $NaM(WO_4)_{2-x}(MoO_4)_x:Eu^{3+}$ (M = Gd Y, Bi), Chem. Phys. Lett. 387 (2004) 2–6.
[9] H. Wu, X. Zhang, C. Guo, J. Xu, M. Wu, Q. Su, Three-band white light from InGaN-based blue LED chip precoated with Green/red phosphors, IEEE Photon. Technol. Lett. 17 (2005) 1160–1162.
[10] R.J. Xie, N. Hirosaki, N. Kiumra, K. Sakuma, M. Mitomo, 2-phosphor-converted white light-emitting diodes using oxynitride/nitride phosphors, Appl. Phys. Lett. 90 (2007) 191101–191103.
[11] C.H. Chiu, C.H. Liu, S.B. Huang, T.M. Chen, Synthesis and luminescence properties of intensely red-emitting $M_5Eu(WO_4)_{4-x}(MoO_4)_x$ (M = Li, Na K) phosphors, J. Electrochem. Soc. 155 (2008) J71–J78.
[12] Q. Zeng, X. Zhang, P. He, H. Liang, M. Gong, Research on rare-earth tungstates red phosphors for white-light emitting diodes, J. Inorg. Mater. 25 (2010) 1009–1014 (in chinese).
[13] Q. Zeng, P. He, M. Pang, H. Liang, M. Gong, Q. Su, $Sr_9R_{2-x}Eu_xW_4O_{24}$(R = Gd and Y) red phosphor for near-UV and blue InGaN-based white LEDs, Solid State Commun. 149 (2009) 880–883.
[14] V.S. Kemmler-Sack, Photoluminescence of trivalent rare earths in perovskite stacking polytypes $Ba_2La_{2-x}RE^{3+}{}_xMgW_2\square O_{12}$ $Ba_6Y_{2-x}RE^{3+}{}_xW_3\square O_{18}$, and $Sr_8SrGd_{2-x}RE^{3+}{}_xW_{4\square}$ O_{24}, Z. Anorg. Allg. Chem. 483 (1981) 126–139.
[15] V.B. Betz, H.J. Schittenhelm, S. Kemmlersa, On ordered perovskites with cationic vacancies. X. Compounds of type $A^{II}{}_2B^{II}{}_{1/4}B^{III}{}_{1/2}M^{VI}O_6 = A^{II}{}_8B_{II}B_2{}^{III}\square M_4{}^{VI}O_6$ with A^{II}, B^{II} = Ba Sr, Ca and MM =$M^{VI=}$U, W, Z. Anorg. Allg. Chem. 484 (1982) 177–186.
[16] V.S. Kemmler-Sack, A. Ehman, On ordered perovskites with cationic tacancies. IX. Compounds of the type $Sr_2Sr_{1/4}B^{III}{}_{1/2}\square WO_6 = Sr_8Sr_1B_{III2}\square W_4O_{24}$ (B^{III} = La, Pr Nd, Sm-Tm, Y), Z. Anorg. Allg. Chem. 479 (1981) 184–190.
[17] R. Zhu, Y. Huang, H.J. Seo, A red-emitting phosphor of Eu-based borotungstate Eu_3BWO_9 for white light emitting diodes, J. Electrochem. Soc. 157 (2010) H1116–H1120.
[18] H. Lin, Y. Huang, H.J. Seo, The red luminescence characteristics of fully concentrated Eu-based phosphor $EuBaB_9O_{16}$, Phys. Stat. Sol. A 207 (2010) 1210–1215.
[19] C.A. Kodaira, H.F. Brito, M.C.F.C. Felinto, Luminescence investigation of Eu^{3+} ion in the $RE_2(WO_4)_3$ matrix (*RE* = La and Gd) produced using the Pechini method, J. Solid State Chem. 171 (2003) 401–407.
[20] S. Ye, C.H. Wang, Z.S. Liu, J. Lu, X.P. Jing, Photoluminescence and energy transfer of phosphor series $Ba_{2-z}Sr_zCaMo_{1-y}W_yO_6$:Eu, Li for white light UVLED applications, Appl. Phys. B 91 (2008) 551–557.
[21] K.R. Reddy, K. Annapurna, S. Buddhudu, Fluorescence spectra of $Eu^{3+}:Ln_2O_2S$ (Ln = Y, La, Gd) powder phosphors, Mater. Res. Bull. 31 (1996) 1355–1359.
[22] Z.L. Wang, H.B. Liang, M.L. Gong, Q. Su, Luminescence investigation of Eu^{3+} activated double molybdates red phosphors with scheelite structure, J. Alloys Compd. 432 (2007) 308–312.
[23] Z. Sun, G. Cao, Q. Zhang, Y. Li, H. Wang, Thermal stable Eu-doped $CaTiO_3$ phosphors with morphology-control for high-power tricolor white LEDs, Mater. Chem. Phys. 132 (2012) 937–942.
[24] V. Sivakumar, U.V. Varadaraju, A promising orange-red phosphor under near UV excitation, Electrochem. Solid-State Lett. 9 (2006) H35–H38.
[25] V. Sivakumar, U.V. Varadaraju, Synthesis, phase transition and photoluminescence studies on Eu^{3+}-substituted double perovskites-A novel orange-red phosphor for solid-state lighting, J. Solid. State Chem. 181 (2008) 3344–3351.
[26] Z. Xia, J. Sun, H. Du, D. Chen, J. Sun, Luminescence properties of a new green emitting Eu^{2+}-doped barium chlorosilicate phosphor, J. Mater. Sci. 45 (2009) 1553–1559.
[27] S. Ye, C.H. Wang, X.P. Jing, Photoluminescence, Raman spectra of double-perovskite $Sr_2Ca(Mo/W)O_6$ with A- and B-site substitutions of Eu^{3+}, J. Electrochem. Soc. 155 (2008) J148–J151.
[28] X. Zhang, Z. Li, H. Zhang, S. Ouyang, Z. Zou, Luminescence properties of $Sr_2ZnWO_6:Eu^{3+}$ phosphors, J. Alloys Compds. 469 (2009) L6–L9.
[29] G. Blasse, Luminescence and Energy Transfer, Structure and Bonding vol. 42, Springer, Berlin, 1980, pp. 1–43.
[30] G. Blasse, On the Eu^{3+} fluorescence of mixed metal oxides. IV. The photoluminescent efficiency of Eu^{3+}–ctivated oxides, J. Chem. Phys. 45 (1966) 2356–2361.
[31] A.C. Van der Steen, J.T.W. De Hair, G. Blasse, Energy transfer between octahedral tungstate and uranate groups in oxides with perovskite structure, J. Lumin. 11 (1976) 265–269.